

Atomic structures and energies of partial dislocations in wurtzite GaN

J. Kioseoglou, G. P. Dimitrakopoulos, Ph. Komninou,* and Th. Karakostas

Department of Physics, Aristotle University of Thessaloniki, GR-54124 Thessaloniki, Greece

(Received 18 December 2003; revised manuscript received 5 March 2004; published 16 July 2004)

The atomic structures of $1/6(20\bar{2}3)$ partial dislocations delineating the I_1 intrinsic basal stacking fault in wurtzite GaN are modelled using an empirical interatomic potential in combination with anisotropic elasticity calculations. Twelve stable configurations are obtained for each polarity, and their core radii, energies, and atomic configurations are given. The 5/7-atom ring core in which the atoms are tetrahedrally coordinated is found energetically favorable among the edge dislocation configurations. For the mixed type partials, 5/7- and 12-atom rings are obtained as low-energy cores, but none of them is found to comprise only tetrahedrally coordinated atoms. Each of them is found energetically favorable under distinct structural conditions.

DOI: 10.1103/PhysRevB.70.035309

PACS number(s): 61.72.Ff, 61.72.Nn, 34.20.Cf, 71.55.Eq

I. INTRODUCTION

Transmission electron microscopy observations show that epitaxial GaN films contain large numbers of line and extended defects mainly threading and misfit dislocations, inversion domain boundaries, and stacking faults (SFs).^{1,2} Such defects are introduced mainly due to the generalized (structural, thermal) mismatch between the epilayer and the substrate, which is usually sapphire but may also be SiC, Si, GaP, etc.³ In order to improve epilayer quality, buffer layers are commonly employed to mediate misfit relief. High defect densities are observed at or near such layers comprising many SFs delimited by partial dislocations. It has been shown that the prevalent SF⁴⁻⁶ is the I_1 intrinsic one.⁷

The influence of dislocations on the electrical, optical, and mechanical properties of Ga-based III-nitride semiconductors is currently under intense investigation. Efficient optical devices such as blue-light-emitting diodes are commercially available despite the presence of a high density ($\sim 10^9$ cm⁻²) of threading dislocations.³ Initial theoretical results using *ab initio* calculations indicated that charge-neutral edge and screw threading dislocations do not contribute to gap states and they are electrically inactive.⁸ Other *ab initio* studies have shown that edge dislocations may be charged, giving rise to deep-gap states.^{9,10} Dependence of the core formation energies on the Fermi level and growth stoichiometry has also been examined.⁹ Moreover tight binding calculations have shown evidence for empty gap states associated with edge dislocations in the top half of the gap.¹¹ More recently, new structures for the screw dislocation have been proposed under certain growth conditions.^{12,13} In addition, by the use of first-principles calculations of electron energy-loss spectra, another study has shown gap stages associated with edge dislocations.¹⁴

Besides the perfect lattice dislocations, optoelectronic properties of devices should be also influenced by the partial dislocations when they exist in large numbers. The aim of the present contribution is to perform a systematic investigation of the core structures and the corresponding energies of the $1/6(20\bar{2}3)$ edge and mixed partial dislocations that bound I_1 intrinsic basal stacking faults in wurtzite GaN, from which an understanding of their influence on optoelectronic proper-

ties may be developed. Core radii and energies are evaluated in an approach combining anisotropic elasticity and atomistic calculations. Initially, the dislocation displacement field is imposed according to anisotropic elasticity theory, and the system is then relaxed to the minimum energy. Such an approach has been applied in the past on dislocations in a variety of materials.¹⁵⁻¹⁷ For our purpose, a modified empirical Stillinger-Weber potential¹⁸ is employed in the atomistic calculations; this potential has been found suitable to describe line and extended defects in GaN.^{17,19-22} The use of an empirical potential in order to describe the structures and energetics of dislocations is certainly less accurate in comparison with a tight-binding approach or *ab initio* calculations, since it does not consider explicitly the electronic effects.

Tight-binding or *ab initio* calculations employ mainly two approaches in order to model dislocations. In the first approach, a dislocation dipole or multipole is placed in a supercell and this leads to a considerable interaction between dislocations. In the second approach, in which an isolated dislocation is considered in a supercell cluster with periodic boundary conditions along the dislocation line and hydrogen-terminated surfaces parallel to the line direction, the long-range elastic effects are not treated rigorously.^{14,16,23} On the other hand, however, in dislocation modeling, medium and long-range strain effects play an important role and the empirical potential offers better embedding of the core into the surrounding bulk material. The advantages of the empirical potential calculations are the competency to treat more than 15 000 atoms and the efficient way to take into account fixed boundary conditions in surfaces parallel to the line direction of the dislocation far from the core area. The strain induced by the dislocation in this case is more accurately estimated, and, since the stress of the supercell geometry influences the core structure and the core energy,²⁴ it provides a better embedding of the core. Moreover, such calculations have been proven²⁵ suitable for treating relatively complicated supercells comprising planar defects.

In Sec. II, the I_1 SF and its bounding partial dislocations are described. In Sec. III, the computational method is given, and the results of its application to the partial dislocation core configuration are analyzed in Sec. IV. In Sec. V, dislocations' core radii and energies are calculated. The potential

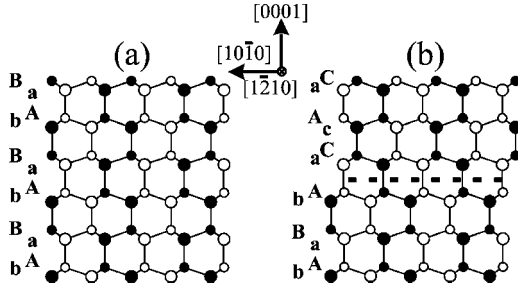


FIG. 1. (a) Wurtzite structure and (b) I_1 SF projected along the $\langle 1\bar{1}0 \rangle$ direction. The broken line indicates the SF plane, large and small circles denote distinct atomic species, unfilled circles are at 0 level, and filled circles are at level $a/2$ along the projection direction.

influence of these partial dislocations on the electrical properties is discussed, and the conclusions are given in Sec. V.

II. THE I_1 STACKING FAULT IN WURTZITE GaN

GaN commonly adopts the wurtzite structure (space group $P6_3mc$),²⁶ which comprises four atoms per unit cell and can be visualized as two interpenetrating hexagonal substructures; one of Ga and one of N atoms related by the distance u along the c axis. With primitive vectors $\mathbf{a}_1 = (\frac{1}{2}, -\sqrt{3}/2, 0)a$, $\mathbf{a}_2 = (\frac{1}{2}, \sqrt{3}/2, 0)a$, and $\mathbf{a}_3 = (0, 0, c/a)a$ in Cartesian coordinates, the positions of the atoms, in units of \mathbf{a}_1 , \mathbf{a}_2 , and \mathbf{a}_3 , are $(\frac{1}{3}, \frac{2}{3}, 0)$ and $(\frac{2}{3}, \frac{1}{3}, \frac{1}{2})$ for atoms of the one species, and $(\frac{1}{3}, \frac{2}{3}, u)$ and $(\frac{2}{3}, \frac{1}{3}, u + \frac{1}{2})$ for atoms of the other species. The stacking sequence along $[0001]$ is ...AaBbAaBbAaBb..., i.e., each layer parallel to the basal plane is composed of two sublayers of distinct atomic species (aB or bA, where capital and small fonts denote distinct atomic species) [Fig. 1(a)].

In the wurtzite structure, two types of intrinsic SFs, designated I_1 and I_2 , and one extrinsic, designated E, can be formed.⁷ These are low-energy defects since they do not disturb the nearest-neighbor packing. The I_1 intrinsic SF [Fig. 1(b)] corresponds to one violation of the stacking rule and can be formed by the removal of a B plane followed by shearing by $1/3\langle 10\bar{1}0 \rangle$ (Fig. 2).

In order to describe the I_1 SF configuration with bounding partial dislocations, we start from the perfect crystal.⁷ Upon removal or addition of a basal disk of atoms (vacancy or interstitial disk) and assuming that only displacements normal to the basal plane are associated with the precipitation, the SF is bounded by a Frank loop with Burgers vectors $1/2[0001]$.⁷ A loop of Shockley partial dislocation is then nucleated in the faulted region leading to the formation of I_1 SF. In other words, if a shear is associated with vacancy

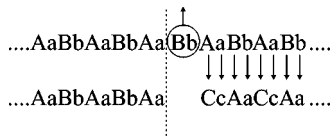


FIG. 2. The stacking sequence in the formation of a I_1 SF.

(case a) or interstitial disk precipitation (case b), the I_1 type fault could be formed. The above SFs are bounded by loops comprising edge and mixed segments with Burgers vectors

$$\mathbf{b}_e = 1/2[0001] + 1/3[10\bar{1}0] = 1/6[20\bar{2}3]$$

and

$$\mathbf{b}_m = 1/2[0001] + 1/3[1\bar{1}00] = 1/6[2\bar{2}03],$$

respectively (assuming a $[1\bar{1}0]$ segment line direction).

III. COMPUTATIONAL METHOD

Atomic configurations (supercells) of each dislocation model were created in the form of rectangular parallelepiped volumes with edges along the $[1\bar{1}0]$, $[10\bar{1}0]$, and $[0001]$. The size of the parallelepiped was $4 \times a$ along $[1\bar{1}0]$, $24 \times c$ along $[0001]$ and $23 \times a 3^{1/2}$ along $[10\bar{1}0]$ (where a and c are the equilibrium lattice parameters) and contain a total of 16 000 atoms.

The supercells initially contained perfect crystal of wurtzite GaN. By employing displacements expected from anisotropic elasticity theory,⁷ the unrelaxed structures of the I_1 intrinsic SF and the corresponding partial dislocation were formed to be used as initial atomic positions. Each supercell contained one partial at its center with line direction $[1\bar{1}0]$; the partial separated the faulted from the unfaulted part of the supercell. The dislocation line was taken to be defined by the symmetry center of one of the two interpenetrating hexagonal substructures. Periodic boundary conditions were applied along $[1\bar{1}0]$, while fixed boundaries were imposed along the other two directions. For the calculations, the modified¹⁷ Stillinger-Weber potential (MSWp) has been employed. The calculations of the minimum energy configurations were performed using the quench molecular dynamics method.²⁷ Generally, atomistic empirical potential calculations provide the total energy of a relaxed structure. Let $E_{\text{TOTAL}}^{\text{excess}}$ be the total excess energy of a supercell, defined as the difference between the total energy found by empirical potential calculations and the energy of a supercell of perfect GaN crystal containing the same number of atoms. Let also E_{SF} be the SF energy per unit area, i.e., the total excess energy of a supercell containing the planar defect divided by planar defect area. E_{SF} was evaluated by relaxing a supercell containing a I_1 SF in the middle; periodic boundary condition were employed along all three directions. The I_1 SF formation energy was found equal to $1.8 \text{ meV}/\text{\AA}^2$ compared to $1.1 \text{ meV}/\text{\AA}^2$ given by *ab initio*;²⁸ i.e., the MSWp provided the energy in satisfactory agreement with the *ab initio* calculations.

The energy per unit length $E_d(R)$ of each partial dislocation in a cylinder of radius R was calculated as the total excess energy of the cylinder minus the SF energy (which is equal to the E_{SF} multiplied by the SF area in the cylinder). Hence,

$$E_d(R) = \frac{E_{\text{TOTAL}}^{\text{excess}}(R) - E_{\text{SF}}[\text{SF}_{\text{area}}(R)]}{L}, \quad (1)$$

where L is the length of the supercell along $[1\bar{1}0]$.

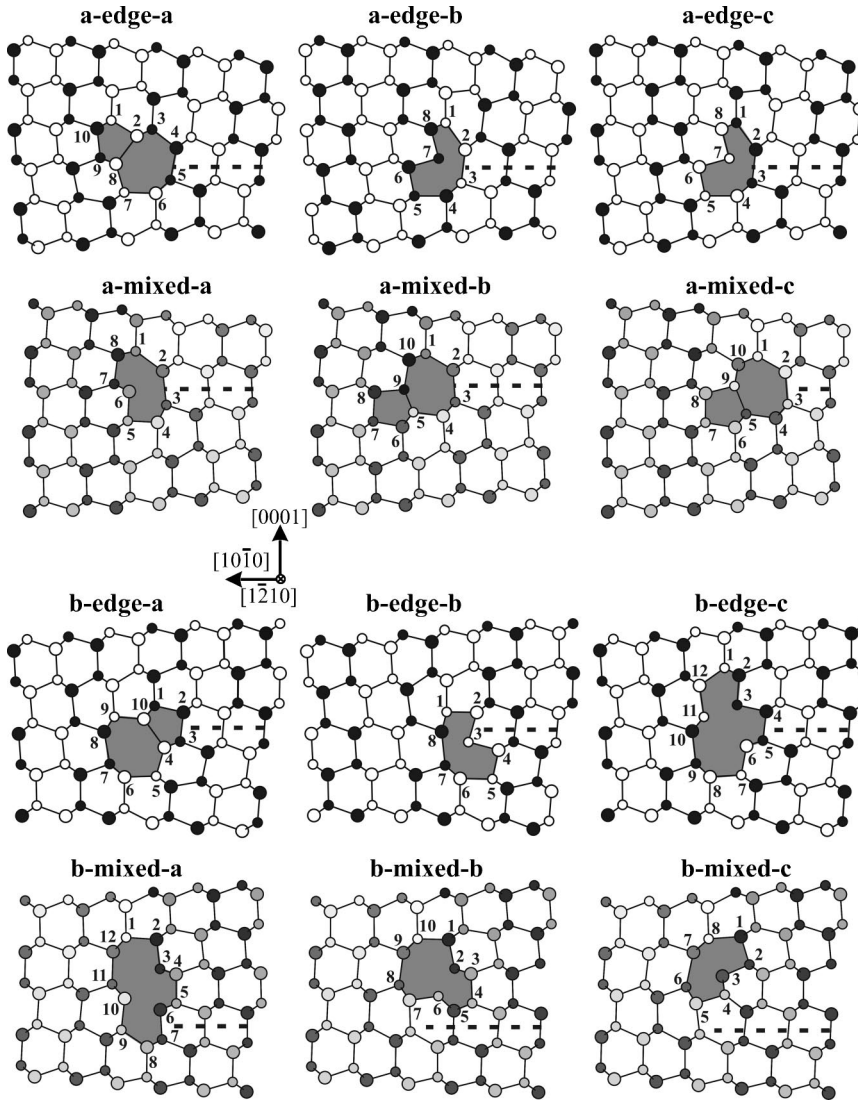


FIG. 3. The relaxed atomic core configurations in N-polarity GaN projected along the $[1\bar{1}2]_{10}$ direction. Symbols are as in Fig. 1. Shading of atoms indicates distinct levels along the projection direction. For the edge dislocations there are two such levels (i.e., at 0 and $a/2$), whereas for mixed type partials, shading denotes multiple different levels. The shaded atomic rings depict the cores of the dislocations.

IV. PARTIAL DISLOCATIONS' CORE CONFIGURATIONS

As mentioned in Sec. II, the I_1 SF can be considered to be formed from a collapsed vacancy disk (case a) or a precipitated interstitial loop (case b) followed by a shear. For each configuration, the shear may lead to either an edge or a mixed type partial dislocation. For the $[1\bar{1}2]_{10}$ line direction, the edge dislocation is $\mathbf{b}_e = 1/6[2\bar{0}2\bar{3}]$ and the mixed $\mathbf{b}_m = 1/6[2\bar{2}0\bar{3}]$. In Fig. 3, the fully relaxed core structures of all the admissible atomic configurations are presented. Since, in $[0001]$ orientation, the wurtzite structure presents two polarities (N or Ga polarity), each atomic configuration is relaxed in both cases. In all atomic configurations we have assumed bonds between atoms within distances up to 2.4 \AA , which is the range of the MSWp for the N-N interaction (although the range for Ga-N and Ga-Ga interactions is larger than 3 \AA).¹⁷ In the following, the configurations obtained for cases a and b are discussed in detail for both polarities.

A. Case (a): I_1 SF obtained from a collapsed vacancy disk

In Fig. 3, a-edge-a is the relaxed atomic configuration obtained for the edge partial dislocation. A 5/7-atom ring is

obtained in which all the atoms are fourfold coordinated. This core does not exhibit any dangling bond, although it comprises a “wrong” bond (bond between atoms 2 and 8, which are of the same atomic species). In order to eliminate the wrong bond, removal (or addition) of one atomic column is necessary. Upon removal of one atomic column from the a-edge-a configuration, the vacancy core structure shown in a-edge-b is obtained. The a-edge-c core configuration is the interstitial structure formed by the addition of a column of atoms. Both the a-edge-b and the a-edge-c configurations exhibit an 8-atom ring comprising an atom with coordination number 2 (atom 7 in Fig. 3, a-edge-b and c).

In Table I, we present the bond lengths and bond angles (minimum, maximum, average) of the core atoms of the a-edge relaxed configurations in N-polarity material, whereas in bold face we present the variation of each value due to the reversal of the polarity. In wurtzite GaN the equilibrium bond length is 1.96 \AA and the equilibrium bond angle is 109.47° . Each value changes when we inverse the polarity of each atomic configuration, and we present the significantly large variations (larger than 0.07 \AA for bond lengths and larger than 5° for bond angles). In the a-edge-a configuration, atoms 2 and 8, which are bounded by a wrong bond,

TABLE I. Bond lengths and bond angles for the core atoms of the a-edge relaxed configurations in N-polarity GaN. In boldface type the variation of each value due to the reversal of the polarity (i.e., Ga polarity) is presented for variations larger than 0.07 Å for bond lengths and larger than 5° for bond angles. Atom numbers refer to Fig. 3.

		a-edge-a					
		Bond lengths (Å)			Bond angles (°)		
Atom		Min	Max	Av	Min	Max	Av
1	N	1.88	1.93	1.91	105- 6	119+ 9	110
2	Ga	1.91- 0.29	2.24- 0.27	2.00- 0.13	84+ 13	119	109
3	N	1.91	1.97	1.94	104	1.24- 7	110
4	Ga	1.97	2.10	2.01	100	117	109
5	N	2.01	2.10	2.04	99	119	109
6	Ga	2.03	2.03	2.03	92	117	110
7	N	1.91	2.03	1.97	101	118	109
8	Ga	1.91- 0.29	2.24- 0.29	2.00- 0.14	99	127+ 8	109
9	N	1.89	1.93	1.91	105- 6	114	109
10	Ga	1.89	1.91	1.90	103	114	109

		a-edge-b					
		Bond lengths (Å)			Bond angles (°)		
Atom		Min	Max	Av	Min	Max	Av
1	N	1.89	2.13	1.96	97	144	109
2	Ga	2.06	2.17- 0.11	2.10	89	137	108
3	N	1.99	2.17- 0.11	2.05	100	117	109
4	Ga	2.02	2.05	2.03	91	118	110
5	N	1.90	2.05	1.96	101	119	109
6	Ga	1.90	2.01	1.94	95	114	109
7	N	1.95	2.01	1.98	91	91	91
8	Ga	1.89	1.95	1.91	95	124	109

		a-edge-c					
		Bond lengths (Å)			Bond angles (°)		
Atom		Min	Max	Av	Min	Max	Av
1	N	1.89	2.13	1.96	97	144	109
2	Ga	2.05	2.16- 0.11	2.10	89	137	108
3	N	1.99	2.16- 0.11	2.05	100	117	109
4	Ga	2.02	2.05	2.03	91	118	110
5	N	1.90	2.05	1.96	101	119	109
6	Ga	1.90	2.01	1.94	94	114	109
7	N	1.95	2.01	1.98	91	91	91
8	Ga	1.89	1.95	1.91	95	124	109

present the largest variations in bond lengths and angles, while their neighboring atoms 1 and 9 present a significant variation in bond angles. In the a-edge-b and c configurations, atoms 2 and 3 present the largest variations in maximum bond lengths due to their neighborhood with the low coordinated atom 7.

Regarding the a-mixed configurations, the initial relaxed atomic configuration, a-mixed-a, presents an 8-atom ring in which atom 3 is low coordinated and has a dangling bond. Upon removal or addition of a column of atoms, the vacancy

or interstitial configurations a-mixed-b and c are formed, respectively. Both of them present 5/7-atom rings, but in the c configuration, the core is shifted with respect to the b model along the $[10\bar{1}0]$ direction. Note that in a-mixed-b the initial column of inversion centers that defines the dislocation line (see Sec. III) passes through the 7-atom ring, whereas in a-mixed-c, it passes through the 5-atom ring. In the a-mixed-b configuration, atom 9 is low-coordinated and exhibits a dangling bond, while in a-mixed-c, atom 10 has coordination number equal to 5. In both configurations, a

TABLE II. Bond lengths and bond angles for the core atoms of the a-mixed relaxed configurations in N-polarity. Notations are as in Table I. Atom numbers refer to Fig. 3.

		a-mixed-a					
		Bond lengths (Å)			Bond angles (°)		
Atom		Min	Max	Av	Min	Max	Av
1	N	1.95	2.17	2.02	97	124	109
2	Ga	1.99	2.21	2.10	95	133	109
3	N	1.99	2.21	2.07	95	127	108
4	Ga	1.97	2.06	2.00	91	127	109
5	N	1.93	1.97	1.94	93- 8	129	109
6	Ga	1.92	1.93	1.93	93	113	106
7	N	1.89	1.93	1.92	98	117	109
8	Ga	1.89	2.00	1.95	98	123	109
		a-mixed-b					
		Bond lengths (Å)			Bond angles (°)		
Atom		Min	Max	Av	Min	Max	Av
1	N	1.94	2.05	1.99	101	120	109
2	Ga	1.99	2.08	2.03	100	124	109
3	N	1.96	2.08	2.01	102	119	109
4	Ga	1.94	2.03	1.98	101	117	109
5	N	1.62+ 0.31	1.99+ 0.32	1.88+ 0.17	95- 19	120+ 12	109
6	Ga	1.91	1.99	1.95	97+ 7	119	109
7	N	1.92	1.94	1.93	99	122- 7	110
8	Ga	1.91	1.96	1.93	98+ 5	128- 14	109
9	N	1.62+ 0.30	1.96+ 0.36	1.84+ 0.21	103	146- 20	120- 8
10	Ga	1.94	2.01	1.96	105- 7	120	109
		a-mixed-c					
		Bond lengths (Å)			Bond angles (°)		
Atom		Min	Max	Av	Min	Max	Av
1	N	1.99	2.10	2.05	100	120	109
2	Ga	1.98	2.07	2.02	102	124	109
3	N	1.96	2.07	2.00	102	119	109
4	Ga	1.93	2.01	1.98	101	117	109
5	N	1.93	2.31+ 0.09	2.03	77	132	109
6	Ga	1.92	1.96	1.94	100	116	109
7	N	1.88	1.93	1.91	99	118	109
8	Ga	1.88	2.00	1.93	97	126	109
9	N	2.00	2.31+ 0.09	2.14	92	152	110
10	Ga	2.04	2.22+ 0.12	2.09	68	144	106

“wrong” bond between atoms of the same species (atoms 9 and 5) occurs. In Table II we present the bond lengths and bond angles of the core atoms of the a-mixed relaxed configurations in N-polarity, and in boldface type the variation of these values for Ga-polarity material. In the a-mixed-a configuration, the only significant variation is the minimum angle of atom 5 that is bonded with the low coordinated atom 6. In a-mixed-b and c configurations, considerable variations are observed in wrong bonded atoms 9 and 5. In the b configuration, significant angle variation occurs in atom 8,

which is bonded with the low-coordinated atom 9, while in the c configuration, the over-coordinated atom 10 presents significant variation in maximum bond length.

B. Case (b): I₁ SF obtained from a precipitated interstitial loop

In Fig. 3, b-edge-a is the relaxed atomic configuration obtained for the edge partials. As in the a-edge-a case, a 5/7-atom ring is again observed with all the atoms being

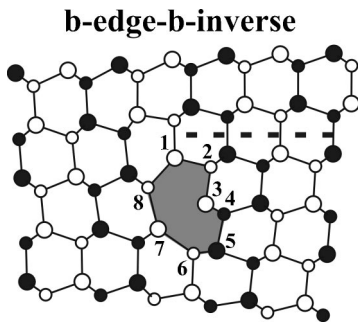


FIG. 4. The b-edge-b relaxed atomic core in Ga-polarity GaN viewed along $\langle 1\bar{2}10 \rangle$. Symbols are as in Fig. 1.

fourfold coordinated. The core comprises a wrong bond between atoms 10 and 4 (Fig. 3). Upon addition or removal of a column of atoms, the interstitial or vacancy configurations b-edge-b and b-edge-c, respectively, are formed. The b-edge-b configuration exhibits an 8-atom ring, including an atom with coordination number 2 (atom 3). The b-edge-b core in Ga-polarity exhibits a quite different configuration. As shown in Fig. 4, the 8-atom ring is shifted along $[000\bar{1}]$ by $\sim c/2$ and is located below the SF plane. In this core structure, two atoms (1 and 3) are low-coordinated and exhibit dangling bonds.

In the b-edge-c configuration, a 12-atom ring is observed exhibiting two atoms with coordination number equal to 3 (atoms 6 and 11) and an atom with coordination number 2 (atom 3). The distances between atoms 3 and 11, and between 3 and 6, are found much larger than 2.4 \AA in both polarities, and consequently no bonds between them are assumed. In Table III, we present the bond lengths and bond angles of the core atoms for the b-edge relaxed configurations. Significant variations are observed due to the reversal of the polarity in the b-edge-a configuration in atoms 4 and 10, which are bound by the wrong bond. In addition, in atoms 1 and 3, variation occurs in bond angles due to their neighbourhood with the wrong bonded atoms.

In the b-mixed-a configuration, the initial relaxed core structure is presented. A 12-atom ring is observed exhibiting three atoms with coordination number equal to 3 (atoms 3, 6, and 10). The distances between these three atoms are found much larger than 2.4 \AA in both polarities and consequently no bonds between them are assumed. By adding a column of atoms, the interstitial configuration b-mixed-b is found. In the b-mixed-b core, a 10-atom ring is observed having two atoms with coordination number equal to 3 (atoms 2 and 6) and one atom with coordination number 5 (atom 5). In addition, in this case, the distance between atoms 2 and 6 is larger than 2.4 \AA and hence we do not assume a 5/7-atom ring. Upon adding one more atomic column in the b-mixed-b core, the b-mixed-c configuration is obtained. In the b-mixed-c core an 8-atom ring is observed in which atom 3 is low-coordinated and presents a dangling bond. In Table IV we present the bond lengths and bond angles of the core atoms for the b-mixed relaxed configurations. Significant variations occur in the b-mixed-b core in nontetrahedrally coordinated atoms 5 and 6. In b-mixed-c core, noteworthy variations occur primarily in atom 4 and secondarily in the

bond lengths of atoms 6 and 7 and in the bond angles of atoms 2 and 8 due to their neighborhood with the low-coordinated atom 3.

V. PARTIAL DISLOCATIONS' CORE RADII AND ENERGIES

Continuum elasticity theory is complementary to atomistic simulations for the modeling of line defects since it allows an evaluation of the long-range strain effects, whereas atomistic simulations describe core structure and energy. The strain energy of an infinite straight dislocation in a perfect crystal can be calculated analytically using linear elasticity.⁷ The total energy of a dislocation is equal to the elastic energy plus the core energy:

$$E_{\text{total}} = E_{\text{elastic}} + E_{\text{core}}. \quad (2)$$

The elastic energy per unit length of a dislocation contained in a cylinder of radius R is given by

$$E_{\text{elastic}} = A \ln \frac{R}{r_0}, \quad r_0 \leq R, \quad (3)$$

where $A = Kb^2/4\pi$ is the prelogarithmic factor, \mathbf{b} is the Burgers vector, K is an energy factor, and r_0 is the core radius.

Let xz be the basal plane where x is $[10\bar{1}0]$, and let the dislocation line $[1\bar{2}10]$ coincide with the z axis. The y axis in this coordinate system is along the $[0001]$ direction. The elastic energy of a dislocation in the basal plane can be decomposed into screw and edge parts according to anisotropic elasticity as follows:⁷

$$E_{\text{elastic}} = \frac{1}{4\pi} (K_s b_s^2 + K_{e_x} b_{e_x}^2 + K_{e_y} b_{e_y}^2) \ln \frac{R}{r_0}, \quad (4)$$

where K_s is the energy factor of b_s , the screw component of the Burgers vector of the dislocation, and K_{e_x} , K_{e_y} are the energy factors of the edge components, b_{e_x} and b_{e_y} , respectively.

The energy factors are equal to⁷

$$K_s = (C_{44}C_{66})^{1/2}, \quad (5)$$

$$K_{e_x} = [(C_{11}C_{33})^{1/2} + C_{13}] \left\{ \frac{C_{44}[(C_{11}C_{33})^{1/2} - C_{13}]}{C_{33}[(C_{11}C_{33})^{1/2} + C_{13} + 2C_{44}]} \right\}^{1/2}, \quad (6)$$

and

$$K_{e_y} = [(C_{11}C_{33})^{1/2} + C_{13}] \left\{ \frac{C_{44}[(C_{11}C_{33})^{1/2} - C_{13}]}{C_{11}[(C_{11}C_{33})^{1/2} + C_{13} + 2C_{44}]} \right\}^{1/2}, \quad (7)$$

where C_{11} , C_{13} , C_{33} , C_{44} , and C_{66} are elastic constants.

As has been shown in the second section, two types of admissible partial dislocations may bound the I_1 SF. An edge dislocation with Burgers vector equal to $\mathbf{b}_e = 1/6[20\bar{2}3]$ and a mixed type dislocation with Burgers vector $\mathbf{b}_m = 1/6[2\bar{2}03]$. In both cases the dislocation line is taken to be

TABLE III. Bond lengths and bond angles for the core atoms of the b-edge relaxed configurations in N-polarity. The values for the b-edge-b configuration are presented in both polarities. Notations are as in Table I. Atom numbers refer to Figs. 3 and 4.

		b-edge-a					
		Bond lengths (Å)			Bond angles (°)		
Atom		Min	Max	Av	Min	Max	Av
1	N	1.89	1.93	1.91	104-7	115+7	109
2	Ga	1.89	1.91	1.90	96	113	109
3	N	1.89	1.93	1.91	105-7	115+7	109
4	Ga	1.91-0.23	2.25-0.28	2.01-0.12	98	128+5	109
5	N	1.91	2.03	1.97	101	118	109
6	Ga	2.03	2.03	2.03	92	117	110
7	N	2.00	2.10	2.04	100	119	109
8	Ga	1.97	2.10	2.01	99	119	109
9	N	1.90	2.03	1.97	98	118	109
10	Ga	1.90-0.23	2.25-0.28	2.00-0.12	99	130	109

		b-edge-b					
		Bond lengths (Å)			Bond angles (°)		
Atom		Min	Max	Av	Min	Max	Av
1	N	1.94	2.06	2.02	91	128	108
2	Ga	1.90	1.99	1.93	75	116	109
3	N	1.99	2.01	2.00	89	89	89
4	Ga	1.90	2.01	1.95	93	114	109
5	N	1.90	2.07	1.97	101	119	109
6	Ga	2.04	2.07	2.05	89	119	110
7	N	1.99	2.18	2.06	102	117	109
8	Ga	2.06	2.18	2.09	87	127	107

		b-edge-b-inverse					
		Bond lengths (Å)			Bond angles (°)		
Atom		Min	Max	Av	Min	Max	Av
1	Ga	1.89	2.03	1.95	105	137	120
2	N	1.89	1.92	1.91	96	113	109
3	Ga	1.90	1.92	1.91	101	112	105
4	N	1.90	1.94	1.92	100	118	109
5	Ga	1.90	1.99	1.96	98	123	108
6	N	1.99	2.19	2.04	95	123	109
7	Ga	2.02	2.19	2.10	103	139	109
8	N	2.00	2.18	2.05	94	124	109

		b-edge-c					
		Bond lengths (Å)			Bond angles (°)		
Atom		Min	Max	Av	Min	Max	Av
1	N	1.90	1.97	1.92	105	125	110
2	Ga	1.90	1.93	1.91	102	116	109
3	N	1.91	1.92	1.92	99	99	99
4	Ga	1.88	1.92	1.91	96	113	109
5	N	1.88	1.94	1.92	104	116	109
6	Ga	1.90	1.94	1.93	106	110	107
7	N	1.90	2.01	1.96	104	117	109
8	Ga	2.01	2.02	2.02	94	115	110
9	N	2.00	2.09	2.04	103	118	109
10	Ga	1.99	2.09	2.02	102	115	109
11	N	1.99	2.03	2.00	107	114	111
12	Ga	1.95	2.03	1.97	102	117	109

[$\bar{1}2\bar{1}0$]. Using the elasticity theory, the prelogarithmic factors for the edge and the mixed dislocations were calculated, as well as the ratio between them. The edge dislocation can be decomposed into two normal edge components $\mathbf{b}_{e_x} = 1/3[10\bar{1}0]$ and $\mathbf{b}_{e_y} = 1/2[0001]$, while the mixed dislocation can be decomposed into a screw $\mathbf{b}_s = 1/6[1\bar{2}10]$ and two normal edge components $\mathbf{b}_{e_x} = 1/6[10\bar{1}0]$ and $\mathbf{b}_{e_y} = 1/2[0001]$. Using elastic constants calculated by the MSWP,²⁹ the prelogarithmic factors are found to be $A_e = 0.79$ and $A_m = 0.73$ eV/Å leading to a ratio equal to $A_e/A_m = 1.08$. If experimental determined elastic constants³⁰ are used the prelogarithmic factors are $A_e = 0.82$ and $A_m = 0.76$ eV/Å, and the ratio between them again equals $A_e/A_m = 1.08$, i.e., due to the satisfactory agreement between the experimental and the calculated elastic constants,²⁹ the obtained prelogarithmic factors are also consistent. The elastic energy of a dislocation is related to the radius of the cylinder and it is infinite for an infinite crystal. Although it can be calculated for a finite radius, it cannot be considered a characteristic invariable property like the core energy. Therefore, only the dislocation core energy, i.e., the energy of the minimum region which cannot be described by elasticity theory, can be used in such capacity.

In order to evaluate the core parameters of dislocations, the energy in the region bounded by coaxial cylinders of radii r and R_0 is plotted versus $\ln(r)$, where R_0 is the external cylinder radius (taken as large as possible), and r is the internal cylinder radius ($r_0 \leq r \leq R_0$). The core radius r_0 is taken at the point where the curve stops being linear. Equation (3) can be written as

$$E_{\text{elastic}}(r) = A \ln R_0 - A \ln r, \quad r \leq R_0. \quad (8)$$

The corresponding prelogarithmic factor is evaluated by fitting Eq. (8) to the calculated values. The core energy is evaluated by averaging the calculated energy values following equation (1) minus the elastic part:

$$E_d(r) - E_{\text{elastic}} = E_d(r) - A \ln r + A \ln r_0, \quad r \geq r_0. \quad (9)$$

Following the procedure described above, Figs. 5 and 6 illustrate the energies $E_{\text{elastic}}(r)$ and $E_{\text{core}}(r) = E_d(r) - E_{\text{elastic}}$ versus $\ln(r)$ plots for partial dislocations delineating a I_1 SF formed by a collapsed vacancy disk or a precipitated interstitial loop, respectively. In all cases, it can be observed that the curve becomes linear and the energy assumes the expression given by elasticity theory [Eq. (8)]. In Table V the calculated core radii, energies, and prelogarithmic factors of the analyzed partial dislocations in both polarities of GaN are given. In addition, the prelogarithmic factors are presented as they have been evaluated by the use of elastic constants calculated with the MSWP ($A_{\text{elastic}}^{\text{MSWP}}$) and by the experimental elastic constants ($A_{\text{elastic}}^{\text{exp}}$).

In the a-edge diagram of Fig. 5, we notice that the 5/7 core is energetically favorable for both polarities and it exhibits the smallest core radius. In the b-edge case, it is found that, as in a-edge case, the 5/7 core configuration has the

lowest energy. These two core configurations are the lowest energy models between all the admissible dislocations and they are the only configurations in which all the atoms are tetrahedrally coordinated. The 8-atom rings (a-edge-b, a-edge-c, and b-edge-b) and the 12-atom ring (b-edge-c) configurations include at least one atom with dangling bond and consequently require higher energies.

In the a-mixed diagram of Fig. 6, it is seen that the a-mixed-b configuration that exhibits a 5/7-atom ring has the smallest core and is energetically favorable. In the b-mixed diagram, it can be seen that the 12-atom ring of the b-mixed-a configuration is energetically favorable and presents the smallest core in comparison with the interstitial type b-mixed-b and c configurations.

Regarding the prelogarithmic factors, the calculated values given in Table V are in agreement with the elasticity theory calculations. Discrepancies occur between the values for vacancy type b-edge-c configuration, and for interstitial type, b-mixed-c configurations and the elastic theory calculated values. This divergence is related to the fitting process, in particular in determining the exact value where the curves become linear.

In closing this section, we remark that the obtained cores are structurally similar to those found favorable for perfect basal dislocations in GaN by *ab initio* calculations,^{23,31} as will be further discussed in the following section.

VI. DISCUSSION AND CONCLUSIONS

In recent *ab initio* calculations of 60° perfect basal dislocations in GaN,^{23,31} with Burgers vector $\mathbf{b}_m = 1/3[2\bar{1}10]$, core structures have been proposed comprising similar 5/7-, 8-, and 12-atom rings similar to our results. In the referenced *ab initio* study,^{23,31} all the possible atomic core configurations have been found electrically active, with a band induced close to the valence band maximum, which can be expected to act as an acceptor in *p*-type GaN in accordance with cathodoluminescence studies on basal perfect dislocations.³² Both these perfect dislocations and the mixed type partial dislocations treated here have the same screw component i.e., ($\mathbf{b}_s = 1/6[1\bar{2}10]$), whereas the edge component along $\langle 10\bar{1}0 \rangle$ is $1/2[10\bar{1}0]$ and $1/6[10\bar{1}0]$ for the perfect and the partial dislocations, respectively, and the partial also comprises an additional $1/2[0001]$ edge component. Although the core structures are not identical (since the Burgers vectors are different), the two cases may be compared. As in the 60° perfect dislocations,^{23,31} our 5/7- and 8-atom rings (cases a-mixed-b and a-mixed-a, respectively) contain a dangling bond, whereas the 12-atom ring (case b-mixed-a) contains three atoms with coordination number equal to 3. Our 5/7-atom ring vacancy configuration (a-mixed-b) has been found to require 0.3 eV/Å less energy than the initial 8-atom ring (case a-mixed-a), in agreement with Blumenau *et al.*²³ Moreover, the Ga-Ga wrong bond in the 5/7-atom ring is equal to 2.31 Å compared to 2.37 Å in perfect dislocations.²³ Regarding the 8-atom ring, the average bond length for the low-coordinated atom has been determined to be 1.82 Å and

TABLE IV. Bond lengths and bond angles for the core atoms of the b-mixed relaxed configurations in N-polarity. Notations are as in Table I. Atom numbers refer to Fig. 3.

		b-mixed-a					
		Bond lengths (Å)			Bond angles (°)		
Atom		Min	Max	Av	Min	Max	Av
1	N	1.98	2.05	2.01	95	120	109
2	Ga	1.91	1.99	1.95	101	125	109
3	N	1.91	1.94	1.93	100	111	106
4	Ga	1.88	1.94	1.91	98	117	109
5	N	1.88	1.94	1.92	99	117	109
6	Ga	1.93	1.94	1.93	96	110	104
7	N	1.91	1.94	1.93	98	115	109
8	Ga	1.91	2.00	1.95	100	122	109
9	N	1.95	2.05	1.99	97	118	109
10	Ga	1.99	2.05	2.02	105	121	111
11	N	1.99	2.10	2.03	102	121	109
12	Ga	1.98	2.10	2.03	102	122	109
		b-mixed-b					
		Bond lengths (Å)			Bond angles (°)		
Atom		Min	Max	Av	Min	Max	Av
1	Ga	1.91	2.03	1.97	98	127	109
2	N	1.91	1.95	1.93	101	112	108
3	Ga	1.89	1.95	1.92	96	117	109
4	N	1.89	2.07	1.97	97-5	119	109
5	Ga	1.90	2.15+0.17	2.03+0.09	64+9	141	105
6	N	1.89	2.15+0.17	2.03+0.12	99-10	121	109
7	Ga	1.89	2.02	1.97	96	123	109
8	N	1.95	2.12	2.02	98	123	109
9	Ga	1.99	2.12	2.05	102	126	109
10	N	1.99	2.09	2.03	92	124	110
		b-mixed-c					
		Bond lengths (Å)			Bond angles (°)		
Atom		Min	Max	Av	Min	Max	Av
1	Ga	1.91	2.10	1.98	90	128	109
2	N	1.91	1.93	1.92	98-6	126	109
3	Ga	1.91	2.01	1.97	92	107	102
4	N	1.93	2.20-0.08	2.03	84+7	144-13	107
5	Ga	1.93	2.05	1.99	96	127	108
6	N	1.96	2.31-0.16	2.07	97	125	109
7	Ga	2.01	2.31-0.16	2.11	95	129	109
8	N	2.02	2.10	2.07	88-8	127	110

the average angle is 114° , while the bonds of the other atoms of the core are expanded by 7%,^{23,31} In our a-mixed-a case, the average bond length for the low-coordinated atom is 1.94 \AA and the average angle is 103° , while the bonds of the other core atoms are expanded by 5%. Furthermore, in our 12-atom ring (case b-mixed-a), the distances between the

three low-coordinated atoms are 2.55 \AA between Ga atoms and 2.63 \AA , 3.84 \AA between Ga and N atoms, while in the perfect dislocation case the distances are 2.5 \AA between Ga atoms and 3.33 \AA , 3.66 \AA between Ga and N atoms.^{23,31}

Based on the above discussion, it is reasonable to postulate that $1/6\langle 20\bar{2}3 \rangle$ partial dislocations in wurtzite GaN may

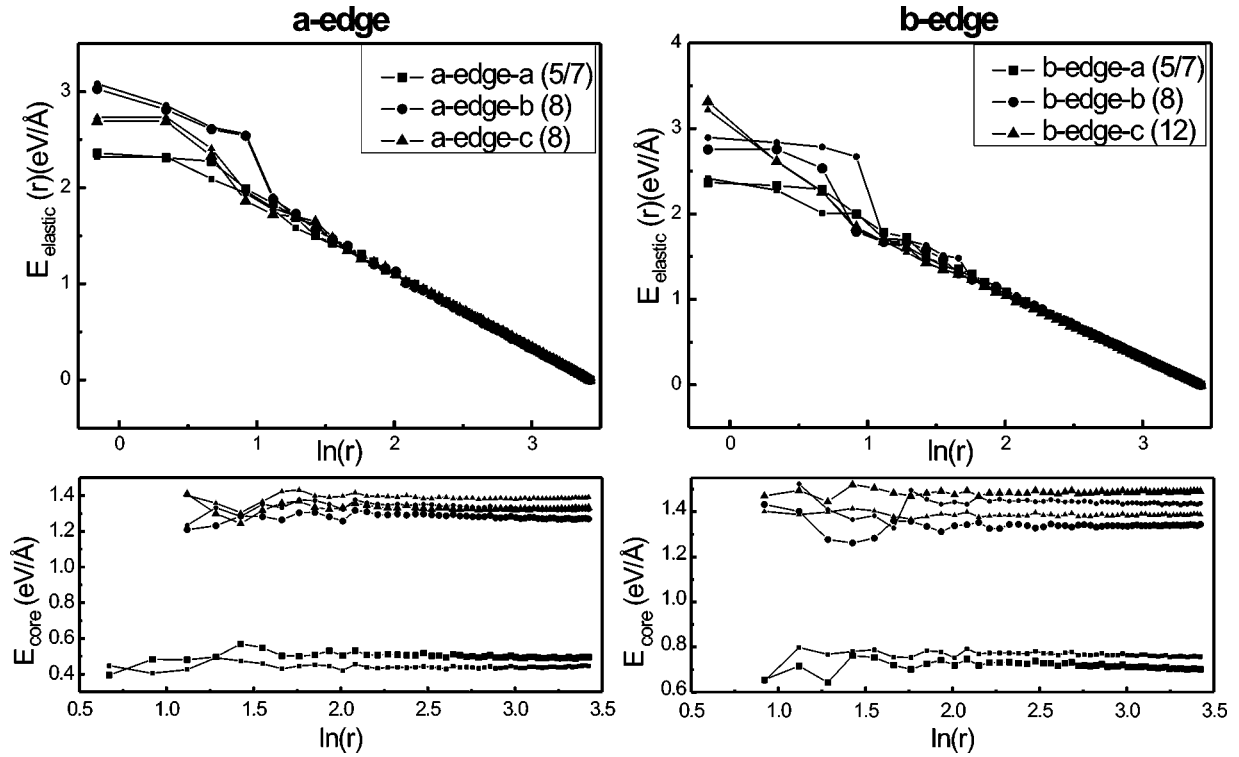


FIG. 5. Elastic energy per unit length $E_{\text{elastic}}(r)$ stored in the region bounded by coaxial cylinders of radii r and R_0 , and the core energy $E_{\text{core}}(r) = E_d(r) - E_{\text{elastic}}$ as a function of $\ln(r)$ for the a-edge and b-edge configurations. (Large symbols denote N-polarity, whereas small symbols denote Ga-polarity.) The core radius r_0 is given by the radius below which linearity breaks down.

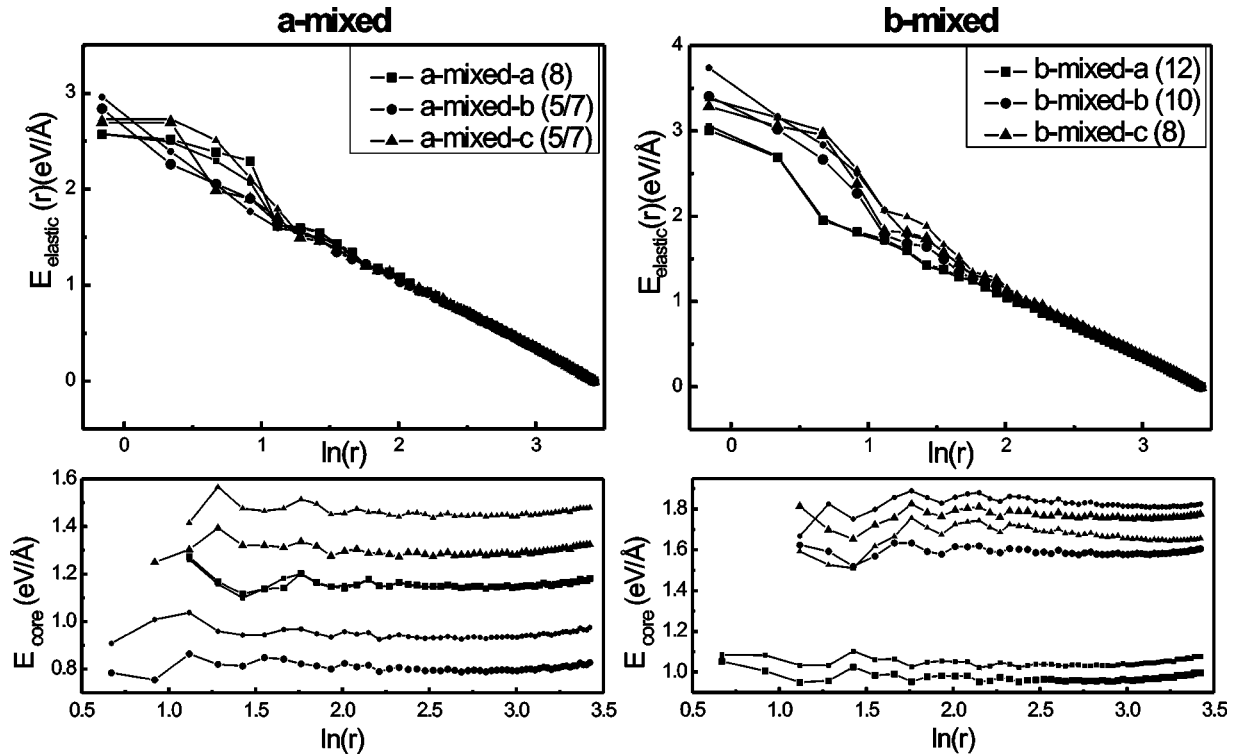


FIG. 6. Elastic energy per unit length $E_{\text{elastic}}(r)$ stored in the region bounded by coaxial cylinders of radii r and R_0 , and the core energy $E_{\text{core}}(r) = E_d(r) - E_{\text{elastic}}$ as a function of $\ln(r)$ for the a-mixed and b-mixed configurations. Symbols are as in Fig. 5.

TABLE V. The calculated core radii, energies, and prelogarithmic factors of the $1/6\langle 20\bar{2}3 \rangle$ partial dislocations of GaN in N-polarity. The values for Ga-polarity are given in parentheses. The prelogarithmic factors obtained from anisotropic elasticity by the use of MSWp-calculated elastic constants ($A_{\text{elastic}}^{\text{MSWp}}$) and by the use of experimental elastic constants ($A_{\text{elastic}}^{\text{exp}}$) are given.

Partial dislocation	Core configuration	r_0 (Å)	E_{core} (eV/Å)	A (eV/Å)	$A_{\text{elastic}}^{\text{MSWp}}$ (eV/Å)	$A_{\text{elastic}}^{\text{exp}}$ (eV/Å)
a-edge-a	5/7	2.0 (2.0)	0.50±0.02 (0.45±0.01)	0.79 (0.76)	0.79	0.82
a-edge-b	8	3.1 (3.1)	1.28±0.02 (1.34±0.02)	0.79 (0.79)	0.79	0.82
a-edge-c	8	3.1 (3.1)	1.34±0.02 (1.39±0.02)	0.78 (0.78)	0.79	0.82
b-edge-a	5/7	2.5 (2.5)	0.72±0.02 (0.76±0.02)	0.78 (0.76)	0.79	0.82
b-edge-b	8	2.5 (3.1)	1.34±0.02 (1.43±0.03)	0.75 (0.78)	0.79	0.82
b-edge-c	12	2.5 (2.5)	1.48±0.01 (1.39±0.01)	0.73 (0.73)	0.79	0.82
a-mixed-a	8	3.1 (3.1)	1.17±0.02 (1.17±0.02)	0.74 (0.74)	0.73	0.76
a-mixed-b	5/7	2.0 (2.0)	0.81±0.02 (0.96±0.02)	0.73 (0.72)	0.73	0.76
a-mixed-c	5/7	2.5 (3.1)	1.30±0.02 (1.48±0.02)	0.73 (0.75)	0.73	0.76
b-mixed-a	12	2.0 (2.0)	0.99±0.02 (1.05±0.02)	0.73 (0.72)	0.73	0.76
b-mixed-b	10	3.1 (3.1)	1.60±0.02 (1.83±0.03)	0.78 (0.83)	0.73	0.76
b-mixed-c	8	3.1 (3.1)	1.77±0.03 (1.66±0.04)	0.81 (0.87)	0.73	0.76

contribute band gap states. However, in addition to the core structure, the strain environment in the surrounding crystal plays an important role. Further investigations are required in order to determine their influence on the band structure.

In conclusion, we have systematically modeled the $1/6\langle 20\bar{2}3 \rangle$ partial dislocations in wurtzite GaN using anisotropic elasticity theory and empirical potential calculations. Our calculations reveal twelve stable configurations in each polarity and their core structures have been presented. The core radii, energies, and the prelogarithmic factors have been calculated by plotting the elastic energy contained in two coaxial cylinders versus $\ln(r)$. Although there are difficulties in determining the exact cylinder radius below which linearity breaks down, the core radii have been calculated in the range between 2 and 3.1 Å, and, in all cases, the smallest cores belong to the energetically favorable configurations.

The 5/7 ring core in which the atoms are tetrahedrally coordinated has been found energetically favorable among the edge configurations; such cores have been calculated, in all cases, to have energies less than 0.76 eV/Å. The 8- and 12-atom rings have been found to require energies from 1.28 to 1.48 eV/Å.

Regarding the mixed type partial dislocations, a variety of core configurations (8-, 5/7-, and 12- atom rings) has been

revealed. The 5/7- and 12-atom ring configurations have been found favorable for partial dislocations, delineating a I_1 SF formed by a collapsed vacancy disk or a precipitated interstitial loop, respectively. However, none of them has been found to consist of only tetrahedrally coordinated atoms. Their core energies are larger than the edge type dislocations, and the energetically favorable models were found to require energies from 0.81 to 1.05 eV/Å.

The empirical potential calculations have been also employed to determine prelogarithmic factors of the partial dislocations, in satisfactory agreement with anisotropic elasticity theory, thus confirming the coherency of the calculations.

The majority of the dislocation core structures possessed either dangling bonds or highly distorted bond angles and lengths. Since reduced coordination or strained bonds contribute to the introduction of gap states,^{11,23} such dislocations could be electrically active. Furthermore the core stress field could act as a trap for electrically active native defects (e.g., vacancies) or impurities.

ACKNOWLEDGMENTS

This work was supported by PENED 01ED481 project of the GSRT.

*Corresponding author. Electronic address: komnhnoy@auth.gr

¹J. L. Rouvière, M. Arlery, B. Daudin, G. Feuillet, and O. Briot, *Mater. Sci. Eng.*, B **50**, 61 (1997).

²Ph. Komninou, Th. Kehagias, J. Kioseoglou, E. Sarigiannidou, Th. Karakostas, G. Nouet, P. Ruterana, K. Amimer, S. Mikroulis, and A. Georgakilas, in *GaN and Related Alloys 2000*, edited by U. Mishra, M. S. Shur, C. M. Wetzel, B. Gil, and K. Kishino, MRS Symposia Proceedings No. 639 (Materials Research Society, Pittsburgh, 2001), G3.47.

³J. I. Pankove and T. D. Moustakas, in *Semiconductors and Semimetals*, edited by R. K. Willardson and E. R. Weber (Academic, New York, 1998), Vols. 50–57.

⁴N. E. Lee, R. C. Powell, Y. W. Kim, and J. E. Green, *J. Vac. Sci. Technol. A* **13**, 2293 (1995).

⁵X. H. Wu, L. M. Brown, D. Kapolnek, S. Keller, B. Keller, S. P. DenBaars, and J. S. Speck, *J. Appl. Phys.* **80**, 3228 (1996).

⁶V. Potin, P. Ruterana, and G. Nouet, *J. Phys.: Condens. Matter* **12**, 10301 (2000).

- ⁷J. P. Hirth and J. Lothe, *Theory of Dislocation*, 2nd ed. (Wiley, New York, 1982).
- ⁸J. Elsner, R. Jones, P. K. Sitch, V. D. Porezag, M. Elstner, Th. Frauenheim, M. I. Heggie, S. Oberg, and P. R. Briddon, *Phys. Rev. Lett.* **79**, 3672 (1997).
- ⁹A. F. Wright and U. Grossner, *Appl. Phys. Lett.* **73**, 2751 (1998).
- ¹⁰K. Leung, A. F. Wright, and E. B. Stechel, *Appl. Phys. Lett.* **74**, 2495 (1999).
- ¹¹S. M. Lee, M. A. Belkhir, X. Y. Zhu, Y. H. Lee, Y. G. Hwang, and T. Frauenheim, *Phys. Rev. B* **61**, 16 033 (2000).
- ¹²J. E. Northrup, *Appl. Phys. Lett.* **78**, 2288 (2001).
- ¹³J. H. Northrup, *Phys. Rev. B* **66**, 045204 (2002).
- ¹⁴C. J. Fall, R. Jones, P. R. Briddon, A. T. Blumenau, T. Frauenheim, and M. I. Heggie, *Phys. Rev. B* **65**, 245304 (2002).
- ¹⁵M. Heggie and M. Nysten, *Philos. Mag. B* **50**, 543 (1984).
- ¹⁶A. T. Blumenau, M. I. Heggie, C. J. Fall, R. Jones, and T. Frauenheim, *Phys. Rev. B* **65**, 205205 (2002).
- ¹⁷A. Bere and A. Serra, *Phys. Rev. B* **65**, 205323 (2002).
- ¹⁸F. Stillinger and T. A. Weber, *Phys. Rev. B* **31**, 5262 (1985).
- ¹⁹J. Kioseoglou, G. P. Dimitrakopoulos, H. M. Polatoglou, L. Lymperakis, G. Nouet, and Ph. Komninou, *Diamond Relat. Mater.* **11**, 905 (2002).
- ²⁰J. Kioseoglou, H. M. Polatoglou, L. Lymperakis, G. Nouet, and Ph. Komninou, *Comput. Mater. Sci.* **27**, 43 (2003).
- ²¹J. Kioseoglou, Ph. Komninou, G. P. Dimitrakopoulos, Th. Kehagias, H. M. Polatoglou, G. Nouet, and Th. Karakostas, *Solid-State Electron.* **47**, 553 (2003).
- ²²A. Bere, and A. Serra, *Phys. Rev. B* **66**, 085330 (2002).
- ²³A. T. Blumenau, C. J. Fall, J. Elsner, R. Jones, M. I. Heggie, and T. Frauenheim, *Phys. Status Solidi C* **0**, 1684 (2003).
- ²⁴X. Blase, K. Lin, A. Canning, S. G. Louie, and D. C. Chrzan, *Phys. Rev. Lett.* **84**, 5780 (2000).
- ²⁵M. Kohyama, *Modell. Simul. Mater. Sci. Eng.* **10**, R31 (2002).
- ²⁶S. Strite and H. Morkoç, *J. Vac. Sci. Technol. B* **10**, 1237 (1992).
- ²⁷L. Verlet, *Phys. Rev.* **159**, 98 (1967).
- ²⁸C. Stampfl and C. G. Van de Walle, *Phys. Rev. B* **57**, R15 052 (1998).
- ²⁹N. Aichoune, V. Potin, P. Ruterana, A. Hairie, G. Nouet, and E. Paumier, *Comput. Mater. Sci.* **17**, 380 (2000).
- ³⁰A. Polian, M. Grimsditch, and J. Grzegory, *J. Appl. Phys.* **79**, 3343 (1996).
- ³¹J. Elsner, A. T. Blumenau, T. Frauenheim, R. Jones, and M. I. Heggie, *MRS Symposia Proceedings No. 595* (Materials Research Society, Pittsburgh, 2000), W9.3.1.
- ³²M. Albrecht, H. P. Strunk, J. L. Weyher, I. Grzegory, S. Porowski, and T. Wosinski, *J. Appl. Phys.* **92**, 2000 (2002).